DOE/PC/95231-24
Dist. Category UC-112
UTSI-99-04

TOPICAL REPORT

DRAFT

DEVELOPMENT OF *IN-SITU* CONTROL DIAGNOSTICS FOR APPLICATION OF EPITAXIAL SUPERCONDUCTOR AND BUFFER LAYERS

Work Performed Under Contract No. DE-AC-22-95PC95231--24

Prepared by:

B. C. Winkleman
T. V. Giel, Jr.
J. Cunningham

University of Tennessee Space Institute
B. H. Goethert Parkway
Tullahoma, TN 37388-8897

June 1999

Table of Contents

List of Figures

Number Page

List of Tables

Number Page

1.0 Executive Summary

The recent achievements of critical currents in excess of $1x10^6$ amp/cm^2 at 77K in YBCO deposited over suitably textured buffer/substrate composites have stimulated interest in the potential fabrication of these “coated conductors” as “wire”. Numerous approaches and manufacturing schemes for producing coated conductor wire are currently being developed. Recently, under the U. S. Department of Energy (DOE’s) sponsorship, the University of Tennessee Space Institute (UTSI) performed an extensive evaluation of leading coated conductor processing options [(1)]. In general, it is our feeling that the science and chemistry that are being developed in the coated conductor wire program now need proper engineering evaluation to define the most viable options for a commercial fabrication process. All fabrication processes will need process control measurements. This report provides a specific review of the needs and available technologies for process control for many of the coated conductor processing options. This report also addresses generic process monitoring areas in which additional research and development is needed. The concentration is on the two different approaches for obtaining the textured substrates that have been identified as viable candidates. These are the Los Alamos National Laboratory’s (LANL) ion-beam assisted deposition, called IBAD, to obtain a highly textured yttria-stabilized zirconia (YSZ) buffer on nickel alloy strips, and Oak Ridge National Laboratory’s (ORNL) rolling assisted, bi-axially textured substrate option called RABiTS™.

2.0 Introduction

Small laboratory samples of coated high temperature superconductors have shown superior performance to particulate-based high temperature superconductors in that they can have higher critical fields and temperatures. [2,3] Only coated conductors using YBCO are considered in this study. The YBCO material has a characteristic critical current of the order of 1.0×10^6 A/cm^2 when observed on single crystals of the parent material. In a multi-crystalline structure, the critical current density is drastically reduced by the presence of crystalline boundaries, but it is possible to grow YBCO films maintaining a high order, or texture, such that a highly aligned crystalline matrix having low angle grain boundaries results. When this is successfully accomplished the film intergranular critical current density approaches the film intragranular current density. Typical YBCO films are only of the order of a few microns thick, when they are called "thick" films, and are deposited on a metallic strip as thin as 1 mil (25 μm).

One of the biggest hurdles to widespread application of YBCO coated conductor wire is developing a manufacturing process that will produce them in long lengths and at prices competitive to copper for applications such as motors, generators, *etc.* In fact, most coated conductors have only been produced in a laboratory environment with a characteristic area of a few square centimeters. Thus, there presently is no infrastructure for making long length coated conductors, like there is to make long length particulate based high temperature superconductors. (Particle based superconductors are primarily made by drawing operations, somewhat similar to the methods of producing conventional non-superconducting wire.) However, there are several alternative processes proposed for deposition of highly textured YBCO onto long metallic strips (*i.e.*, coated conductors). UTSI has studied and compared the most commonly known processes, including Pulsed Laser Deposition/Ablation (PLD), Electron Beam (e-beam) based deposition, Metal Organic Chemical Vapor Deposition (MOCVD), the Sol-Gel method, Chemical Vapor Deposition (CVD), Aerosol/Spray Pyrolysis, Metal Organics Decomposition (MOD), Electrodeposition, Electrophoresis, Sputtering, Flash Evaporation and Molecular Beam Epitaxy. [1,4]

In all these methods, appropriate real-time process control diagnostics are needed to maximize resulting superconductor performance. The purpose of the present study is to assess potential process control schemes for the most promising manufacturing processes of coated high temperature superconductors. Process control schemes should enable optimal use of the process materials so that maximum critical fields and temperatures are obtained on a continuous basis, and so that future degradation of wire performance is minimized.

3.0 Description of Typical HTSC Wire/Tape Manufacturing System

In the last few years a major worldwide research effort has been devoted to the Oxide-Powder-In-Tube (OPIT) method to make high-T_c superconducting wires and tapes. However, this OPIT process can only be applied to Bi- or Tl- based oxide superconductors. The sequential and repetitive OPIT operations of mechanical rolling and drawing of the Bi- or Tl- based oxides in silver tubes produces acceptable superconductor quality, while other oxides do not. The oxide $YBa_2Cu_3O_{7-\delta}$ (YBCO) has its irreversibility line at higher temperatures even with a lower superconducting transition temperature as compared to Bi- and Tl- based superconductors, and YBCO will allow applications at 77K and in magnetic fields over 1T if YBCO wire can be made. YBCO is not amenable to the OPIT process, but has proven amenable to deposition on a substrate, as a coated conductor with critical current densities orders of magnitude greater than typical OPIT wire. Thus the development of high-T_c YBCO superconducting films on metallic substrates could be of great value for applications in superconducting magnets, cables, electromagnetic shields, *etc*. Hence researchers trying to develop YBCO based superconductors have been attempting a number of physical and non-physical (*e.g.*, chemical) deposition methods to coat continuous substrate strips.

Under physical methods, the following coated conductor deposition schemes have been evaluated: [1,4]

- Sputter Deposition
  - + Magnetron Sputter Deposition (both RF and DC mode)
  - + Ion-beam Sputter Deposition (both RF and DC mode)

- Electron Beam Evaporation
  - + Co-Evaporation (Using Resistive Heating also)
  - + Activated (Plasma) Reactive Evaporation (Includes Resistive Heating and Ion-Beam Assisted)

- Flash Evaporation

- Plasma Spray

- Molecular Beam Epitaxy (MBE), and

- Laser Ablation (includes Ion-Beam Assisted)

In addition, we have evaluated the following two methods designed to deposit powder in either a slurry or a suspension. [1,4]

- Spin-Casting/Dip-Coating/Screen-Painting, *etc.*

- Electrophoresis

Among the non-physical or chemical or solution-growth techniques, the following methods have been studied: [1]

- Chemical Vapor Deposition (CVD) Techniques
  - + Metallo-organic Chemical Vapor Deposition (MOCVD)
  - + Plasma or Photo-Assisted MOCVD

- Sol-Gel (Spin/Dip-Coating, Spraying, Painting)

- Metal-Organic Decomposition (MOD) [Includes Spin/Dip Coating, Spraying, Painting, *etc.*]

- Electrodeposition, and

- Aerosol/Spray Pyrolysis

Except for the electrophoresis technique evaluated at General Atomics [3], none of the published work started with a metal substrate on one end and ended with the coated material at the other end. In order to develop appropriate conductor coating schemes for the continuous processing/manufacturing of long wires or tapes or ribbons, additional steps that were not tested as part of the deposition scheme need to be included. In general, a spool-to-spool or reel-to-reel type of continuous manufacturing scheme developed for any of the above techniques, would also include at least the following operations:

- preparation of substrate material
- preparation and application of the buffer layer(s)
- preparation and application of the HTS material and required post-annealing, and
- preparation and application of the external protective layer

These four operations are necessary because of the complete match required between the four major components of the finished HTSC wires/tapes. The four major components are substrate, buffer, high temperature superconductor (HTS), and outer protective layer. To evaluate the candidate options for the continuous processing/manufacturing of long length of coated wires, UTSI conceptualized schemes that would incorporate the above deposition schemes and operating steps and thus enable production of long lengths of wire in a reel-to-reel or spool-to-spool mode. [1] Based on the available literature, and from talking to various experts, UTSI was able to put together process schematics for the following options: [1]

- Sol-Gel
- Chemical Vapor Deposition (CVD)
- Metal Organics Chemical Vapor Deposition (MOCVD)
- Metal Organics Decomposition (MOD)
- Electrodeposition
- Electrophoresis
- Aerosol/Spray Pyrolysis
- Pulsed Laser Ablation/Deposition (PLA/PLD)
- Electron Beam-Based Deposition

A suitably textured/crystalline substrate over which layers of buffer material and then the HTS film can be grown in an epitaxial manner is essential for manufacturing coated conductors. Thus the process schematics included the two leading concepts of IBAD and RABiTS[5] for preparing a textured crystalline substrate or substrate-plus-buffer composite.

4.0 Development of Real Time Process Control Using *In-situ* Diagnostics

The various HTSC coated conductor manufacturing processes each require specialized process control measurements. Potential technologies to make the essential measurements need to be identified and investigated. To understand process control needs, analyses of each of the different manufacturing processes are being carried out to determine the type, range, accuracy, *etc.* of required process control measurements. A search for methods that can characterize the quality of the various layers of coated conductors is also being undertaken.

4.1 Process Control Tables

The measurements needed in each process were determined from the process flow schemes given in Reference 1 and from literature surveys [3,6-8], which were undertaken to develop a thorough understanding of each process and a comprehensive tabulation of the control parameters. After the process review, a preliminary worksheet for each process was created to provide a general description of the kinds of measurements needed, as well as noting the parameter ranges when available from the literature. After a satisfactory worksheet for each process was completed the information was tabulated. The resulting partially completed tables follow. The table for each process has six columns denoted “item”, “measurement”, “range”, “accuracy”, “technology”, and “comments”. The “item” column identifies the components or sub-processes, such as dissolver or e-beam based YSZ application (see Table 1. MOCVD METHOD PROCESS CONTROL). The “measurement” column describes what specific measurements will be needed for that item, such as temperature or pressure. The “range” and “accuracy” columns give specifications for the measurement. The information in the “measurement”, “range”, and “accuracy” columns suggests a measurement technique that is presented in the “technology” column. The “comments” column provides questions or comments pertinent to that item.

At the current time these tables provide only some of the necessary information due to the ongoing development of the manufacturing processes and the lack of process details in the open literature. Once completed, these tables will provide valuable information in the further development of the methods by describing processing parameters that must be considered and controlled for the various manufacturing methods.

Table 1 is discussed as an example of the process tables. The first item identified in the table is the substrate. Since a high quality superconductor requires a high quality substrate, it is expected that the substrate quality will require monitoring. The measurements prescribed, such as crystal orientation and morphology, would be needed to properly characterize the substrate quality. Another item listed in the MOCVD Table is the heated piping containing the vapors of yttrium, barium, and copper organic precursors. The precursors must be heated to appropriate temperatures to evaporate and the vapor piping must be heated to prevent condensation but kept below the precursor decomposition temperatures. The different layer applications, such as the e-beam based CeO_2 and YSZ applications and the MOCVD-based HTSC application, also appear in the items column. Pressure, temperature, and deposition rates are some measurements that must be monitored during these applications. The table also identifies process points where measurements such as layer thickness, crystal orientation, and composition of new film layers are required to control layer deposition and ensure quality. The final oxidation/annealing and cooling steps are shown in the table as subprocesses requiring monitoring and control of temperature, time, and oxygen pressure. Where ranges are shown for absolute flow measurements, they must be scaled from the evaluation scale to the manufacturing scale of the deposition facilities.

Near the end of Table 1 two items are included which are not part of the process design. These items are Post Manufacturing Test and Wire Marking System, which have been included in all of the process control tables. The post manufacture testing would provide quality control *via* a thermal quench of the product and subsequent measurement of superconducting electrical characteristics. The wire marking system is included to mark any defect locations detected during manufacture for the purpose of post manufacture processing to remove defective regions.

TABLE 1. MOCVD Method Process Control

Item	Measurement	Range	Accuracy	Technology	Comments
Substrate	crystal orientation				
	morphology				
	geometry				
	grain size				
Annealing Furnace	temperature	900 °C			
Precursor ovens for $Y(DPM)_3$,$Ba(DPM)_2$, $Cu(DPM)_2$	temperature	Y:130-160 °C Cu: 130-160 °C Ba: 260°C (9,10)		oven controls	Avoid thermal decomposition of -DPM precursor vapors. (11)
Pipes inside the gas handling system	temperature	250-300 °C (10)		heating tape	Temperature of pipes containing the Y, Ba, Cu-DPM vapor must be controlled to at least equal the highest -DPM evaporation temperature so -DPM precursors don't condense. (9)
Dissolver	flow rate of $Y(DPM)_3$	75 cm^3/min (10)	1%	mass flow controller	Is this a batch or continuous process?
	flow rate of $Ba(DPM)_2$	600 cm^3/min (10)	1%	mass flow controller	Y:Ba:Cu molar ration in the solution should be 1:4:4 (12)
	flow rate of $Cu(DPM)_2$	80 cm^3/min (10)	1%	mass flow controller	
	solvent flow rate				Molarity of solution should be 0.4 mol/l (12)
	solution level				
Vaporizer	temperature	230 °C			
	vacuum pressure	1-100 Torr		capacitance manometer	
	nitrogen flow rate	50 sccm (12)	1%	mass flow controller	Is this a batch or continuous process?
	precursor solution flow rate	3-6 mm^3/min (12)	1%	mass flow controller	
	vapor species concentration				
E-Beam Based CeO_2 Application	tape temperature				What are the off-gasses?
	flow rate of off-gasses				
	flow rate of H_2/N_2 mix				
	Pressure				
	deposition rate	0.0667 nm/s			
CeO_2 Block	Thickness				When does the block need to be replaced?
	Quality				How is the block obtained?
Film - after CeO_2 application	layer thickness	10 nm			
	crystal orientation				
	Composition				
	Morphology				
	Geometry				
	grain size				
Electron Gun	Power				
	location on target				
E-Beam Based YSZ Application	tape temperature				
	Pressure				
	deposition rate	0.1167 nm/s			
YSZ Block	Thickness				When does the block need to be replaced?
	Quality				How is the block obtained?
Film - after YSZ application	layer thickness	140 nm			
	crystal orientation				
	composition				
	morphology				
	geometry				
	grain size				
MOCVD - Based HTSC Application	temperature	600-850 °C			What are the vapors?
	pressure	1-10 mm Hg		capacitance manometer	
	deposition rate	2 nm/s			
	film temperature	680 °C (12)			
	transport line temperature				
	flow rate of vapors				
Plasma Tube	flow rate of N_2O	250 sccm (12)	1%	mass flow controller	
	flow rate of O_2	50 sccm (12)	1%	mass flow controller	
	power	100 W (12)			
	frequency	13.56 MHz (12)			
Film - after HTSC application	layer thickness	300 nm			
	crystal orientation				
	composition				
	morphology				
	geometry				
	grain size				
Oxidation/Annealing	temperature	460-680 °C		temperature controller	What are the off-gasses?
	time			temperature controller	
	pressure of O_2	100 mm Hg			
	flow rate of off-gasses				
Cooling	temperature	680 down to 25 °C		temperature controller	What are the off-gasses?
	time	65 min (12)		temperature controller	
	pressure of O_2	100 mm Hg			
	flow rate of off-gasses				
Post Manufacturing Test	quenching and I/V characteristics				
Wire Marking System	wire defects				
Global Measurements	speed of ribbon				The speed of the ribbon should control the processing time.
	tension				
	length of ribbon on spool				
	emissions			CEM (continuous emissions monitor)	

TABLE 2. Aerosol/Spray Pyrolysis Method

Item	Measurement	Range	Accuracy	Technology	Comments
Substrate	crystal orientation				
	composition				
	morphology				
	geometry				
	grain size				
Dissolver	flow rates of chemicals				Nitrates should have a 2% concentration (13) Atomic ratio of Y:Ba:Cu of 1:2:3 (14)
Sprayers	temperature	275-400 °C	1% (13)		There are no furnace gradients.
	substrate temperature	200-500°C (15)	1% (13)		
	flow rate of O_2 and N_2	4 l/min (13)			
	deposition rate	138.9 µm/s			
	aqueous nitrates solution delivery rate	1-2 ml/min (13)			O_2/N_2 are in a combined flow.
	Drain/excess spray				
Film - after each sprayer	Layer thickness	200 nm (16)			Final layer thickness of 1000 nm.
	Layer quality				
Preheater	Temperature	600-800 °C			What are the off-gasses?
	Flow rate of off-gasses				
	Flow rate of air				There are no furnace gradients.
Film - after each preheater	Crystal orientation				
	Composition				
	Morphology				
	Geometry				
	Grain size				
Heater	Temperature	850-900 °C		temperature controller	What are the off-gasses?
	Flow rate of O_2 and N_2	4 l/min (13)			
	Flow rate of off-gasses				
	Time	2 hours (13)		temperature controller	
Oxidizer/Cooler	Temperature	500 cooled to 25 °C		temperature controller	What are the off-gasses?
	Time	12 min (13)		temperature controller	Cooling rate of 40 °C/min. (13)
	Flow rate of O_2	4 l/min (13)			
	Flow rate of off-gasses				
Post Manufacturing Test	Quenching & I/V characteristics				
Wire Marking System	Wire defects				
Global Measurements	Speed of ribbon				The ribbon speed should control the processing time.
	Tension				
	Length of ribbon on spool				
	Emissions			CEM (continuous emissions monitor)	

TABLE 3. CVD Method

Item	Measurement	Range	Accuracy	Technology	Comments
Substrate	crystal orientation				
	composition				
	morphology				
	geometry				
	grain size				
Vaporizer #1	temperature	820 °C		temperature controller	States of chemicals? Any corrosive chemicals?
	flow rate of N_2	300 sccm (17)	1%	mass flow controller	
	pressure				
Vaporizer #2	temperature	950 °C		temperature controller	States of chemicals? Any corrosive chemicals?
	flow rate of N_2	150 sccm (17)	1%	mass flow controller	
	pressure				
Vaporizer #3	temperature	340 °C		temperature controller	States of chemicals? Any corrosive chemicals?
	flow rate of N_2	100 sccm (17)	1%	mass flow controller	
	pressure				
Chambers	temperature of pipes to chamber	250 °C (8)		temperature controller	
	deposition rate	83.3 µm/s			
	temperature	750 - 900 °C		temperature controller	
	pressure	20 mm Hg			
	flow rate of O_2	200 sccm (17)			
	flow rate of precursor				
Film - after each chamber	layer thickness				600 nm final layer thickness.
	crystal orientation				
	composition				
	morphology				
	geometry				
	grain size				
Bubbler	temperature	20 °C			Probably will not need to know water flow rate
	flow rate of O_2	200 sccm (17)	1%	mass flow controller	
	level control of water				O_2 / H_2O ratio of 1/7 (17)
Oxidizer/Cooler	temperature	500 °C cooled to 25 °C		temperature controller	What are the off-gasses? Are off-gasses corrosive?
	time	48 hours (17)		temperature controller	
	flow rate of O_2				
	flow rate of off-gasses				
Post Manufacturing Test	quenching & I/V character-istics				
Wire Marking System	wire defects				
Global Measurements	speed of ribbon				The speed of the ribbon controls processing time.
	tension				
	length of ribbon on spool				
	emissions			CEM (continuous emissions monitor)	

TABLE 4. Electrodeposition Method

Item	Measurement	Range	Accuracy	Technology	Comments
Substrate	crystal orientation				
	composition				
	morphology				
	geometry				
	grain size				
Dissolver	flow rate of chemicals				Ba, Cu, Y-nitrates are powders. $AgNO_3$ and HNO_3 are liquids.
	time				
	temperature				
Mixer	flow rates				
	level				
	time				
	quality				
Electrolytic Cell	current density	12 mA/cm^2 (18)			
	voltage	-300 to -500 V (18)			
	electrolyte composition				
Film - after Cell	layer thickness				
	layer quality				
Dryer	temperature	150 °C			What are the off-gasses?
	time				
	flow rate of off-gasses				
Film - after Dryer	crystal orientation				
	composition				
	morphology				
	geometry				
	grain size				
Thermal Treatment	temperature	900-500 °C		temperature controller	What are the off-gasses? O_2 and N_2 are in a combined flow.
	time			temperature controller	
	flow rate of O_2 and N_2				
	flow rate of off-gasses				
Oxidizer/Cooler	temperature	500 °C down to 25 °C		temperature controller	What are the off-gasses?
	time			temperature controller	
	flow rate of cold O_2				
	flow rate of off-gasses				
Post Manufacturing Test	quenching & I/V characteristics				
Wire Marking System	wire defects				
Global Measurements	speed of ribbon				The ribbon speed should control the processing time.
	tension				
	length of ribbon on spool				
	emissions			CEM (continuous emissions monitor)	

TABLE 5. Electrophoresis Method

Item	Measurement	Range	Accuracy	Technology	Comments
Substrate	crystal orientation				
	morphology				
	geometry				
	grain size				
Mixer	flow rates				
	time				
Calciner	temperature	800 - 860 °C (19)		temperature controller	Off-gasses exist?
	time	24 hours (19)		temperature controller	
Pulverizer	flow rate				
	temperature	100 °C			
	particle size				
Slurry Mixers	flow rates				
	levels				
Electrophoresis Chambers	temperature	20 °C (19)	± 4 °C (19)		Any corrosive chemicals?
	current density	5-50 μA/cm^2 (19)			
	voltage	150 V (19)			
	magnetic field	8 T (19)			
	deposition rate	1 - 5 μm/min (19)			
Film (after each chamber)	layer thickness				
	layer quality				
Sintering Furnaces	temperature	900 °C	± 4 °C (19)		What are the off-gasses? Are O_2 and N_2 individual or combined flows? Any corrosive off-gasses?
	flow rates of O_2 and N_2				
	O_2/N_2 ratio				
	flow rate of off-gasses				
Film (after each Furnace)	crystal orientation				
	composition				
	morphology				
	geometry				
	grain size				
Oxidizer/Cooler	temperature	500 °C cooled to 25 °C	± 4 °C (19)	temperature controller	What are the off-gasses? Any corrosive off-gasses?
	time	8 hours (19)		temperature controller	
	flow rate of O_2				
	flow rate of off-gasses				
Post Manufacturing Test	quenching & I/V characteristics				
Wire Marking System	wire defects				
Global Measurements	speed of ribbon				Ribbon speed should control processing time
	tension				
	length of ribbon on spool				
	emissions			CEM (continuous emissions monitor)	

TABLE 6. E-Beam Based Conductor Coating Method Utilizing IBAD Technique for Buffer Application

Item	Measurement	Range	Accuracy	Technology	Comments
Hastelloy Tape	morphology				
	geometry				
Ion Gun	power				
	energy	300 eV (20)			
	current density	200 μA/cm^2 (20)			
	flow rate of argon gas				
E-Beam Based YSZ IBAD Deposition	pressure	4x10^{-4} mm Hg			What are the off-gasses?
	flow rate of off-gasses				At room temperature but substrate temperature increases (23)
	flow rate of O_2				
	deposition rate	0.2 nm/s (21)	1% (22)	atomic absorption monitor (22)	Ion beam must be at 53^o angle to the tape (21)
	substrate temperature	60-100°C (20,23)			
YSZ Block	thickness				When does the block need to be replaced?
	quality				
Electron Gun	power				
	location on target				
Film - after YSZ deposition	layer thickness	10 nm (21)			
	crystal orientation				
	composition				
	morphology				
	geometry				
	grain size				
E-Beam Based YBCO Deposition	pressure	10^{-5} mm Hg			What are the off-gasses?
	flow rate of off-gasses				
	flux density of O	4×10^{16} ions/cm^2-s (21)		silvered quartz crystal thickness monitor (11)	
	deposition rate	10 nm/s	1% (22)	atomic absorption monitor (22)	
	substrate temperature	800 °C (24)			
	atomic absorption rate of Y, Ba, Cu		1% (22)	atomic absorption monitor (22)	
Film - during YBCO deposition	layer thickness	1 μm			
	crystal orientation				
	composition				
	morphology				
	geometry				
	grain size				
YBCO Sources	Thickness				When does this block need to be replaced?
	quality				
Atomic Oxygen Generator	power	100 - 300 W (24)			
	flow rate of O_2	2200 sccm (21)	1%	mass flow controller	
Post Manufacturing Test	quenching & I/V characteristics				
Wire Marking System	wire defects				
Global Measurements	speed of ribbon	3-25 cm/sec (21)			Ribbon speed should control processing time.
	tension				
	length of ribbon on spool				
	emissions			CEM (continuous emissions monitor)	

TABLE 7. MOD (Metalorganic Deposition)

Item	Measurement	Range	Accuracy	Technology	Comments
Substrate	crystal orientation				
	composition				
	morphology				
	geometry				
	grain size				
Dissolver #1	chemical flow rates				Acetates are solid, acid is liquid. Chemicals are corrosive. Y:Ba:Cu acetates in 1:2:3 ratio (25)
	levels				
	temperature	room (25)			
Dryer	time				This is a continuous process. What is output chemical state? Is time sufficient to control quality or is a closed loop required? Chemicals are corrosive.
	temperature	80 °C			
Dissolver #2	chemical flow rates				
	levels				
	temperature	room (25)			
Dip coaters	levels				Chemicals are corrosive.
	precursor solution flow rate				
	deposition rate	2.5 nm/s			
	temperature	23-31 °C (25)			
	composition quality of material in tank				
Film (after each dip coater)	layer thickness				Final thickness of 300 nm.
	layer quality				
Ovens	temperature	200-400°C			What are the off-gasses? The off-gasses are corrosive.
	flow rate of O_2				
	off-gas pressures				
Film (after each oven)	crystal orientation				
	composition				
	morphology				
	geometry				
	grain size				
Decomposer	temperature	850 °C			Gasses are in a combined flow. The off-gasses are corrosive. What is off-gas composition?
	chemical flow rates				
	time				
Oxidizer/Cooler	temperature	500 down to 25 °C		temperature controller	The off-gasses are corrosive. What is off-gas composition?
	flow rate of oxygen				
	time			temperature controller	
Post Manufacturing Test	quenching and I/V characteristics				
Wire Marking System	wire defects				
Global Measurements	speed of ribbon				The speed of the ribbon should control processing time.
	tension				
	length of ribbon on spool				
	emissions			CEM (continuous emissions monitor)	

TABLE 8. PLD Method

Item	Measurement	Range	Accuracy	Technology	Comments
Substrate	crystal orientation				
	morphology				
	geometry				
	grain size				
Mixer	flow rate of powders				Is this a batch process?
	time				Mix 1:4:6 ratio Y_2O_3:$BaCO_3$:CuO
Calciner	temperature			temperature controller	Is this a batch process? Any off-gasses?
	time	24 hrs (26)		temperature controller	Should there be oxygen flow?
Pulverizer	temperature				What type of pulverizer is this?
	time				Is this a batch process?
	flow rate of air				
	particle size				
Annealing Furnace	temperature	900 °C			Need H_2-Ar-gas mix to suppress NiO formation on substrate? (27)
Pulsed-Laser Based YSZ Application	pressure	0.2 mm Hg			What are the off-gasses?
	flow rate of gas mixture				
	deposition rate	0.169 nm/s	1% (22)	atomic absorption (22)	
	tape temperature	790 °C (28)			
YSZ Block	thickness				When to replace block?
	quality				
Laser Beam Generator	power				Assumes XeCl excimer laser
	repetition rate	20 Hz (29)			(λ = 308 nm) (29)
	location on target				
Substrate - after YSZ application	layer thickness	100 nm			
	crystal orientation				
	composition				
	morphology				
	geometry				
	grain size				
Pulsed-Laser Based CeO_2 Application	pressure	0.2 mm Hg			What are the off-gasses?
	flow rate of gas mixture				
	tape temperature	900 °C			
	deposition rate	96.7 µm/s	1% (22)	atomic absorption (22)	
CeO_2 Block	thickness				When to replace the block?
	quality				
Substrate - after CeO_2 application	layer thickness	100 nm			
	crystal orientation				
	composition				
	morphology				
	geometry				
	grain size				
Laser Beam Generator	power				Assumes KrF excimer laser
	repetition rate	10-30 Hz (30, 31)			(λ = 248 nm) (30, 31)
	location on target				
Pulsed-Laser Based YBCO Application	pressure	0.2 mm Hg			What are the off-gasses?
	flow rate of gas mixture				
	tape temperature	800 °C			
	deposition rate	3 nm/s (21)	1% (22)	atomic absorption (22)	
YBCO Block	thickness				Need to sinter and anneal block?
	quality				When to replace the block?
Post Manufacturing Test	quenching & I/V characteristics				
Wire Marking System	wire defects				
Global Measurements	speed of ribbon				Ribbon speed should control processing time.
	tension				
	length of ribbon on spool				
	emissions			CEM (continuous emissions monitor)	

TABLE 9. Sol-Gel Method

Item	Measurement	Range	Accuracy	Technology	Comments
Substrate - RABiTS Ni-rich tape before first buffer dip coating	crystal orientation				
	morphology				
	geometry				
	grain size				
Dissolvers	flow rates of chemicals				What state are the chemicals in? Are the chemicals corrosive?
	time				
	level				
	pressure				
Reflux Distillation #1	flow rates of chemicals				Reflux, distill, dilute until mix reaches boiling point of 124 °C. (32) Sec-butanol goes to recovery. (32)
	temperature	124 °C (32)			
	time				
	level				
	pressure				
Reflux Distillation #2	flow rates of chemicals				Reflux, distill, dilute until mix reaches boiling point of 124 °C. (32) Isopropanol goes to recovery. (32)
	temperature	124 °C (32)			
	time				
	level				
	pressure				
Dilution	flow rates of chemicals				Adjust solution concentration to 0.5 M. (32)
	level				
	temperature				
	pressure				
Partial Hydrolyzer	flow rates of chemicals				Hydrolyze the precursor solution with an equal volume of 1 M H_2O in a 2-methoxyethanol solution. (32)
	level				
	temperature				
	pressure				
Buffer Dip Coaters	level of precursor gel				
	deposition rate	3 nm/s			
	temperature				
Substrate - after each buffer dip coater	layer thickness				Final thickness of 400 nm.
	layer quality				
Pyrolyzers	temperature	800 °C			What are the off-gasses? Are the off-gasses corrosive?
	flow rate of O_2				
	flow rate of off-gasses				
Substrate - after each pyrolyzer	crystal orientation				
	composition				
	morphology				
	geometry				
	grain size				
Dissolvers	flow rates of chemicals				Chemical States? Are chemicals corrosive?
	time				
	level				
	pressure				
Mixer	flow rates of chemicals				Temperature and pressure monitors may not be needed.
	level				
	time				
	pressure				
	temperature				
Vacuum Distillation	flow rates of chemicals				Are chemicals corrosive? Temperature monitor may not be needed.
	pressure				
	time				
	level				
	temperature				
Organic Solution of Precursor	flow rates of chemicals				Are chemicals corrosive? 0.1-0.5 mol solution in a pyridine/ 2-methoxyethanol solvent mixture. (33) May not need temperature monitor.
	level				
	time				
	temperature				
Precursor Dip Coaters	YBCO precursor solution levels				May not need temperature monitor.
	deposition rate	3 nm/s			
	temperature				
Film - after each dip coater	layer thickness				Final thickness of 1000 nm.
	layer quality				
Pyrolyzers	temperature	400 °C			What are the off-gasses?
	flow rate of O_2				
	flow rate of off-gasses				
Film - after each Pyrolyzer	crystal orientation				
	composition				
	morphology				
	geometry				
	grain size				
Thermolyzer	temperature	700 - 850 °C		temperature controller	O_2 and N_2 are in a combined flow. What are the off-gasses?
	flow rates of O_2 and N_2				
	flow rate of off-gasses				
	Time			temperature controller	
Oxidizer/Cooler	temperature	500 down to 25 °C		temperature controller	What are the off-gasses?
	flow rate of O_2	65 $cm^3/min/cm^2$ (33)		mass flow controller	
	flow rate of off-gasses				
	time			temperature controller	
Post Manufacturing Test	quenching & I/V characteristics				
Wire Marking System	wire defects				
Global Measurements	speed of ribbon				Ribbon speed should control processing time.
	Tension				
	length of ribbon on spool				
	Emissions			CEM (continuous emissions monitor)	

4.2 Layer Quality Assessment

A second task in development of real time process control measurements is characterization and quality assessments of the substrate and conductor layers. A number of technologies are available to evaluate the substrate and conductor layer quality, and some are reviewed below. At UTSI X-Ray diffraction (XRD) is being used for *ex-situ* layer characterization of coated conductor samples. With modification XRD may be applicable to *in-situ* layer characterization. Also, potential *in-situ* technologies are actively being investigated for layer quality evaluation including scatterometry, absorption spectroscopy, Raman spectroscopy, and ellipsometry. Study of scatterometry was undertaken due to its potential for surface roughness measurement while absorption spectroscopy is under study as a species flow concentration monitor. Raman spectroscopy is being studied as a means of measuring crystal composition and orientation *in-situ*, and ellipsometry is being studied as a potential *in-situ* layer thickness monitor. Some other techniques which have been used for layer quality evaluations for high temperature superconductor sample fabrication are also briefly discussed.

4.2.1 Surface Roughness

High quality epitaxial growth of superconducting layers on substrates prepared by processes such as RABiTS require smooth substrates. Coated conductor substrates need to have rms surface roughnesses approaching the smoothness optical quality of optical quality surfaces (with rms roughness normally less than 10 nm). This suggests a need for quantifying surface roughness. Microscopy is the standard *ex-situ* technique for quantifying surface roughness, but optical microscopy is limited by the minimum focus of light, due to diffraction, to only detect approximately 1μm or larger surface anomalies. However, atomic force microscopy (AFM) can be used to image surfaces at atomic-scale resolution. AFM uses an atomically-sharp tip that is scanned very close to the surface being measured. The tip is chemically attracted or repulsed by the surface, causing it to move up or down on its supporting cantilever. The AFM tip movement is monitored, typically with laser beam diffraction, as the tip is rastered laterally across the surface to map the surface topography. AFM measurements of adequate RABiTS substrates[3] have shown rms surface roughnesses of 50 nm, but a more rapid, less intrusive technique is needed for *in-situ* surface monitoring during coated conductor manufacturing.

While a surface with rms roughness of 50 nm would be considered a good reflector, exhibiting primarily specular reflection, it would also show significant diffuse scatter. This leads to the potential of scatterometry as a manufacturing diagnostic for determining surface roughness *in-situ*. Measurement of the radiation scattered from a surface can be used to determine many surface roughness parameters such as arithmetic average roughness (s_a), rms roughness (s), average and rms slope parameters (m_a and m), and surface wavelength ($l = 2ps/m$). These parameters can be obtained from the surface power spectral density (PSD) which describes the surface height variations in terms of surface spatial frequencies. The measurable bidirectional scatter distribution function (BSDF), or specifically the bidirectional reflection distribution function (BRDF) for a reflective surface, is related to the surface PSD. Thus measurement of the BSDF allows calculation of surface roughness statistics. The BSDF is the ratio of scattered power (specifically radiance) to illuminating power (or irradiance). It is bidirectional since both the incident and scatter direction are pertinent to the measurement interpretation. The BRDF is also generally two-dimensional (*i.e.*, light is scattered into all directions of the hemisphere above the reflecting surface) since the surface itself is two-dimensional, although the BRDF for an isotropic surface will not depend on the azimuthal angle.

Scatterometers are composed of illumination sources (frequently lasers), a surface holder or positioner, gonimeters, and detector electronics. Because scatterometry is a non-imaging optical technique it can measure surface irregularities which are a fractional size of the illuminating light wavelength. In coated conductor applications, manufacturers need to know the location of surface anomalies so that corrective actions can be taken. Scatterometers will give this information if the laser source is focused to a small spot that is scanned over the surface, but that spot can be scanned considerably faster that an Atomic Force Microscope tip, in part because the spot is orders of magnitude larger than the AFM tip. Multiple detector scatterometers can discriminate between particulate contamination, which can be cleaned off, and surface anomalies, such as pits and voids. Scatterometers

have proven to be fast, reliable thin film and semiconductor wafer surface analyzers, providing data to guide process remediation, and should be amenable to a similar role in coated conductor manufacturing. Figure 1 shows results from an early scatter intensity measurement made at UTSI in different scattering directions over a 0.0625 square inch area of potential coated conductor substrate. In Figure 1 q_S is the altitude scatter angle and f_S indicates forward (0°) and (180°) backward directions. The laser incidence angle was 60°. The scatter intensity normalized between 0 = red (minimum scatter) and 1= purple (maximum scatter) increases when larger surface defects or contaminants like dust are encountered (*e.g.*, q_S = 50°, f_S = 0°). Also, well defined narrow features are obvious at (q_S = 50°, f_S = 180°) and (q_S = 70°, f_S = 180°).

4.2.2Crystal Orientation and Composition

Since achieving high current transport in coated conductors is dependent on elimination of high angle YBCO grain boundaries, sharp biaxial texture of the superconductor coating, of the buffer layers, and perhaps of the substrate (depending on the film deposition method) is required. Appropriate Oxygen and general crystal composition is of course required too, and monitors to measure these parameters *in situ*, in real time need to be developed.

X-ray diffraction (XRD) is the standard *ex-situ* technique for characterization of HTS coated conductors crystal phases, orientations, and orientation distribution (texture sharpness). Also, the same equipment can employ X-ray reflectivity (XRR) to measure film thickness and roughness, provided roughness isn't excessive.

XRD, like other diffraction methods, employs the constructive and destructive interference of electromagnetic radiation after it is split into multiple rays by a "grating" of spacing *d* following Bragg's Law, $n\lambda = 2\,d \sin\theta$, where *n* is an integer, λ is the radiation wavelength, and θ is the angle between the radiation and the surface. Interference occurs only when the physical dimensions being probed are in the same size range as the radiation wavelength, so XRD is useful for examining coated conductor crystal phases and orientations since the crystalline structural features are on the order of the wavelength region of x-rays. Coated conductor samples diffract x-ray beams passing through them to produce intense beams at specific angles depending on the x-ray wavelength, the crystal orientation, and the structure of the crystal. These beams correspond to constructive interference from the atoms which act as diffracting centers, a natural three-dimensional "diffraction grating" to form an assembly of "Laue spots" in sharply defined directions.

Phases are determined by conducting an XRD 2-Θ/Ω scan in which the Bragg/Brentano geometrical relationship between the monochromatic x-ray source, the sample, and the x-ray detector are satisfied. Matching of peak angular positions from a phase scan of the unknown sample with known peak positions of reference phases in the Powder Diffraction File (PDF) database is used to identify phases.

The crystal orientations may be determined from XRD pole figure scans or from Orientation Distribution Function (ODF) plots constructed from pole figure scans.[34] In a pole figure scan, a particular Bragg reflection is scanned by rotating the sample about both its surface normal (Φ rotation) and about an axis lying in both the sample surface and the plane of the x-ray incident and diffracted beams (Ψ rotation). Pole figures for three orthogonal reflections, from which an ODF may be constructed, are sufficient to entirely characterize the phase's preferential crystal orientation with respect to a sample reference plane and direction.

The most used measure of texture sharpness in a coated conductor is the full width at half maximum (FWHM) of an XRD Ω scan peak (for out-of-plane texture) and an XRD Φ scan peak (for in-plane texture). Ω rotation is about an axis lying within the surface plane and normal to the plane of the incident and diffracted x-ray beam (a vertical axis for a horizontal diffractometer).

X-ray diffractometers consist of an x-ray generator, a goniometer and sample holder, and an x-ray detector such as photographic film or a movable proportional counter. The goniometer allows the “Laue spots” to be mapped over a hemisphere using monochromatic beams, and lengthy angular scans of the

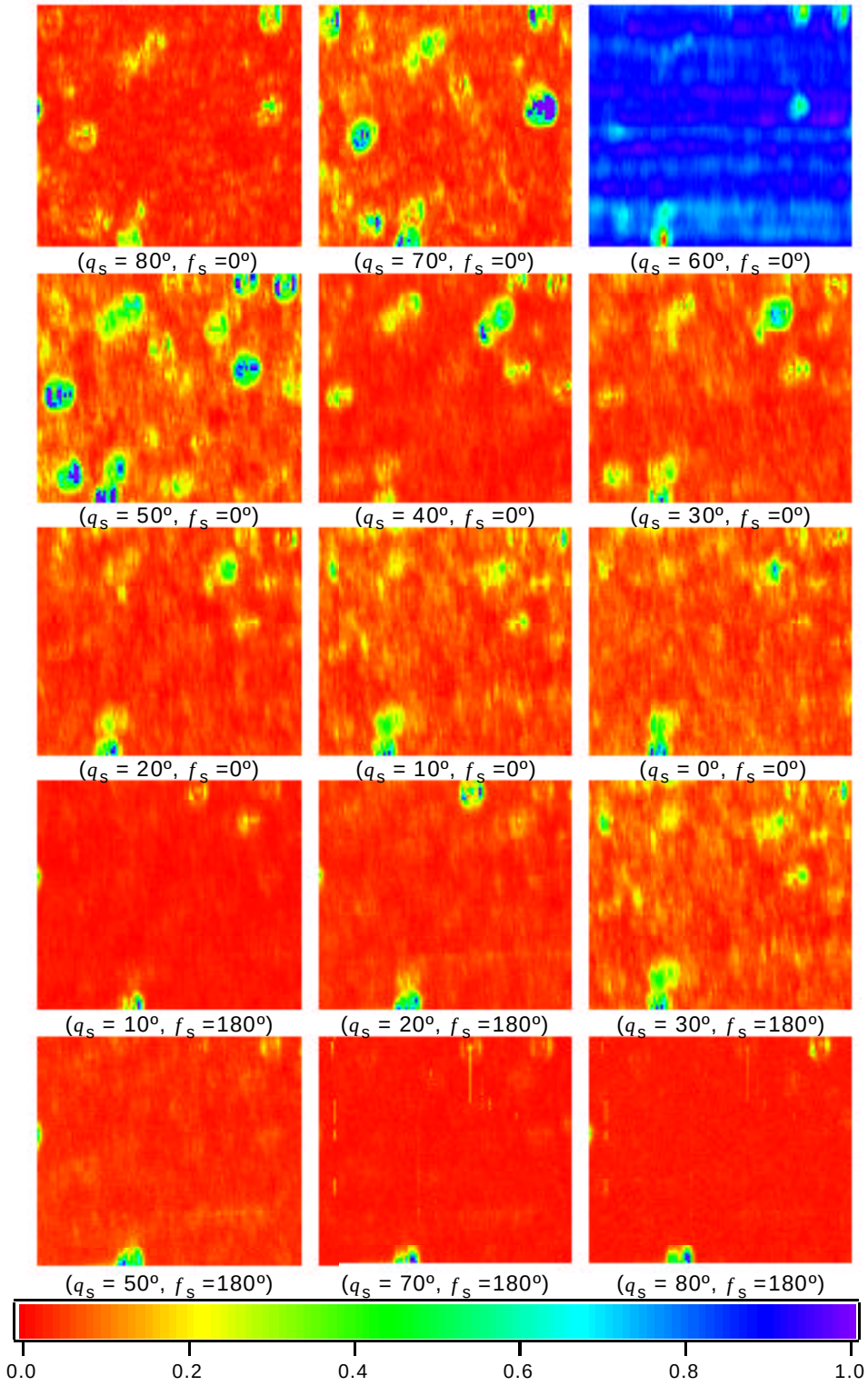

Figure 1. Variation in Scatter Intensity as a Function of Scatter Direction, 60° Laser Incidence Angle.

sample, the detector or both are needed to map out reflections. Thus XRD has not been considered applicable for real time, *in-situ* characterization and process control. However, if energy dispersive diffractometry is employed using white x-ray radiation, a solid-state detector, and a multichannel analyzer, then it is possible with the sample in a fixed geometry to examine texture changes under dynamic conditions.

Reflection High Energy Electron Diffraction (RHEED) diffracts electrons rather than x-ray radiation. Diffraction methods using x-rays, electrons or neutrons have similar wavelength regions of applicability but different penetration depths. Electron diffraction provides only a low penetration depth due to the strong interaction of electrons with the surface, so electron diffraction is usually used in a reflection geometry to study surfaces. RHEED has thus been examined as a potential surface diagnostic. However, electrons scatter from gases so electron diffraction must be performed under vacuum, and most applications of RHEED have been performed near 10^{-6} mbar pressures. [35] Many coated conductor processing schemes are done at higher pressures (*e.g.*, PLD where O_2 background pressures of 0.5 mBar are needed to grow a stable conductor with high texture.) By using a two step differentially pumped electron gun, however, it is possible to perform *in situ* RHEED diagnostics at up to 0.5 mbar, [36,37] during PLD growth of coated conductors for example.

In RHEED a high energy beam (3-100keV) is directed at the sample surface at a grazing angle. The electrons are diffracted by the crystal structure of the sample and then impinge on a phosphor screen mounted opposite to the electron gun resulting in a series of streaks. The distance between the streaks indicates the surface lattice unit cell size. The grazing incidence angle ensures surface specificity despite the high energy of the incident electrons. Atomically flat surfaces result in sharp RHEED patterns but rougher surfaces give a more diffuse RHEED pattern. 'RHEED oscillations' result with variations in surface flatness as a material is “coated” onto a surface. High pressure RHEED should therefore be of particular use as a film growth diagnostic in coated conductor manufacturing.

Parallel Reflection Electron Energy Loss Spectroscopy (PREELS) involves spectral analysis of RHEED electrons to allow real-time measurement of the surface composition in epitaxial film growth. Reflection electron energy loss spectroscopy was pioneered by Dr. H. A. Atwater [38] for *in situ* surface analysis of Si semiconductor epitaxial growth. In PREELS a sample is bombarded with a monoenergetic beam of electrons from a scanning transmission electron microscopy (STEM) which puts out a narrow beam of high energy electrons to probe small regions of the coated conductor and/or substrates. The beam is reflected off the surface resulting in a sharp peak corresponding to elastically scattered electrons, and a number of peaks at lower energy corresponding to excitations of the electron gas in the material. The amount of energy loss identifies the atom that was struck by the beam, giving the surface composition at that “probe” point. However, because the beam is focussed down to the order of the width of an atomic column,[39] detailed scans of whole surfaces during epitaxial superconductor layer growth can be too time consuming for process control.

Raman spectroscopy can measure crystal orientation and composition directly and accurately by measuring vibrational modes in the YBCO crystal. [40-45] Raman spectroscopy is the measurement of the wavelength and intensity of inelastically scattered light from molecules. The Raman scattered light wavelengths are shifted from the incident light by the energies of molecular vibrations. The Raman light intensities are proportional to the frequency and intensity of the incident light as well as the Raman cross section of the molecule. Figure 1 shows a Raman spectroscopy experimental setup used at UTSI for measuring crystal orientation by observing Raman spectra of the HTSC film. Crystal orientation is measured by applying different laser polarizations, using different orientations of the crystal axes and studying different places on the film. [46-49] For example, by comparing the relative intensities of the $500cm^{-1}$ line and the 335 cm^{-1} line in the proper Raman mode, the degree of c-axis tilting from the normal can be determined. [48] YBCO crystal orientation can be determined for YBCO films on a number of substrates with no difficulty. [50]

In laser-based Raman a laser of known frequency is focused onto a sample in order to generate molecular vibrational information in the inelastically scattered Stokes and anti-Stokes bands. These bands contain about 10^{-6} of the scattered light, and they are shifted from the laser input frequency by

vibrational quanta. The vibrational quanta provide an excellent molecular fingerprint of the sample. Raman for relatively large molecules like $YBa_2Cu_3O_{7-x}$ generates rich vibrational spectra which can rapidly identify small changes in the molecular structure. For example, the critical temperature of $YBa_2Cu_3O_{7-x}$ films is dependent upon the oxygen content, which can be monitored with Raman spectroscopy. By observing the 500 cm^{-1} Raman scattering in the proper polarization the oxygen content can be found. [42, 44, 45, 51]

In addition to providing information on crystal orientation and chemical construction, Raman spectroscopy has been used *in situ* to monitor the pulsed laser deposition (PLD) of $YBa_2Cu_3O_{7-x}$ onto various substrates, using an yttria-stabilized zirconia (YSZ) buffer layer. In this configuration, an Nd:YAG laser is used for ablation, and a spectrometer outside the deposition chamber monitors the ablation plume emissions. The spectrometer uses a linear charged-coupled device array with 1024 elements, and emissions are transmitted to the diffraction grating by optical fiber. The spectral refresh rate is on the order of 2 Hz, which is fast enough to assess the quality of the plume. [52]

Raman spectra can generally be generated without sample preparation, is a non-destructive, non-invasive technique, and can be applied via fiber delivery into vacuum chambers or other processing configurations. The recent availability of high-powered diode lasers, inexpensive thermoelectric coolers, charge coupled array detectors, and improved fibers have resulted in commercial Raman system development with compact, rugged and user friendly systems now becoming available. The difficulty using Raman spectroscopy as an *in-situ* diagnostic is the data acquisition speed. Raman spectroscopy must provide real time measurements to be used in a processing environment. However, with technique development, real time measurements should be possible under the appropriate conditions. [41, 46]

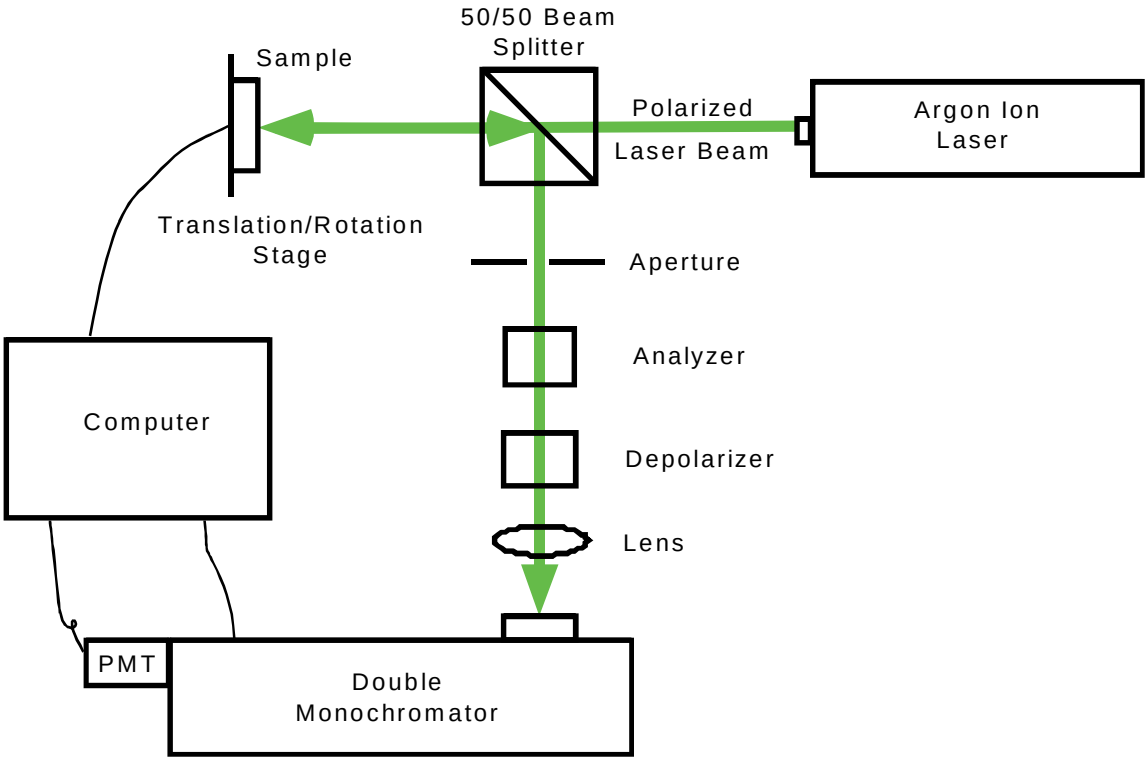

Figure 2. Raman Spectroscopy Setup

4.2.3Flow Rates

YBCO is a complex molecule and growth of YBCO requires stoichiometric flows of the species comprising the YBCO. If bulk YBCO is used as the source, as in PLD, control of flow rates is not required during superconductor deposition. But for growth techniques such as MOCVD which use individual

sources of Y, Ba, Cu and O_2 the flows of these molecules has to be monitored. When the flows are in gas phase (*e.g.*, the copper precursor $Cu(THMD)_2$) the precursor flow rate and species concentration, as well as any carrier gas flow rate, must be monitored to maintain the necessary stoichiometry.

Absorption Spectroscopy is a well known technique for measuring atomic and molecular species concentrations in gas flows.[53] Historically, emission spectroscopy was first applied to characterize species concentrations by qualitative and quantitative analyses of luminescence. In emission spectroscopy, light emitted by thermally excited atoms and molecules is measured. For atoms and simple molecules light is emitted in specific frequency (*i.e.*, wavelength) lines and bands characteristic of the atoms and molecules. Light in these same lines or bands is preferentially absorbed by the atoms and molecules. Absorption spectroscopy is the selective probing to measure absorption of specific lines which identify the species.

In emission spectroscopy light emitted by thermally excited atoms or molecules is measured, but even at high temperatures only a small fraction (determined by the Boltzmann law) of atoms or molecules is excited. The quantity of light absorbed, on the other hand, depends on the number of ground-state atoms, so absorption spectroscopy is more sensitive than emission spectroscopy, and absorption does not thermally destroy fragile molecules (*e.g.*, $Cu(THMD)_2$) like thermal excitation for emission spectroscopy can. Because of the high sensitivity, absorption spectroscopy has become the standard method for accurate measurements of low concentrations of atoms, even in combustion environments where emission lines are generated. Using several different wavelengths, each with a narrow linewidth, allows simultaneous detection of different species concentrations in many cases, making absorption spectroscopy applicable to MOCVD chambers where all precursors coexist, with proper selection of lines.

Typically, atomic absorption spectroscopy has been used to study flame behavior, and for flames of acetylene/oxygen or acetylene/air the sensitivities obtained are in the ppb region,[54] when standard solutions and the standard-addition method is used. For example, the sensitivity in measurements of Ca by atomic absorption in a direct aspiration acetylene/air reducing flame is 80 pico-gram/cc, with a detection limit of 10 pg/cc[55] (or approximately 20 ppb at standard temperature and pressure conditions). However, direct laser excitation of atoms (viz. metallic species) significantly reduces the detection limit to levels well below 1 pg/cc in a graphite furnace burner.[56] Therefore, measurements of atomic concentrations of species such as Y, Ba, and Cu should be possible with a very high sensitivity (1 ppb or better). If significant differences in absorption bands exist for MOCVD precursors $Y(THMD)_3$, $Ba(THMD)_2$ and $Cu(THMD)_2$ their molecular concentrations should also be measurable with high sensitivities, even when mixed. Unfortunately, in absorption spectroscopy studies[57-59] of gas phase and liquid phase MOCVD precursors the absorption bands show significant overlap, with less structure than usually observed for gas phase absorption.[53] Figures 3 and 4 show typical $CU(THMD)_2$ and $Y(THMD)_3$ ultraviolet absorption bands measured at UTSI in typical MOCVD gas phase temperature and vacuum conditions. Therefore, a simultaneous, multi-wavelength measurement scheme needs to be developed to monitor molecular concentrations of $Y(THMD)_2$, $Ba(THMD)_3$ and $Cu(THMD)_2$ in the MOCVD deposition chamber. However, their individual molecular concentrations in the gas feed lines to the deposition chamber should be accurately measurable with single wavelength absorption spectroscopy, in real time for monitoring purposes.

4.2.3 Layer Thickness

Coated conductors are complex layered structures consisting of the substrate, one or several buffer layers, the superconductor layer, and an inerting layer. The performance of the final conductor is dependent on the thicknesses of each layer, and in particular, the engineering current density of the conductor is a direct function of the combined thickness of all the layers as well as the thickness of the YBCO layer. Therefore, it is important to monitor the thicknesses of each layer as they are deposited. This is particularly true for techniques like Sol-Gel that can create different layer thicknesses depending on how they are drawn through the gel, as well as gel thickness and composition. (Gel composition also needs to be monitored *in situ*, and Raman is a candidate technique for that real time process monitoring.)

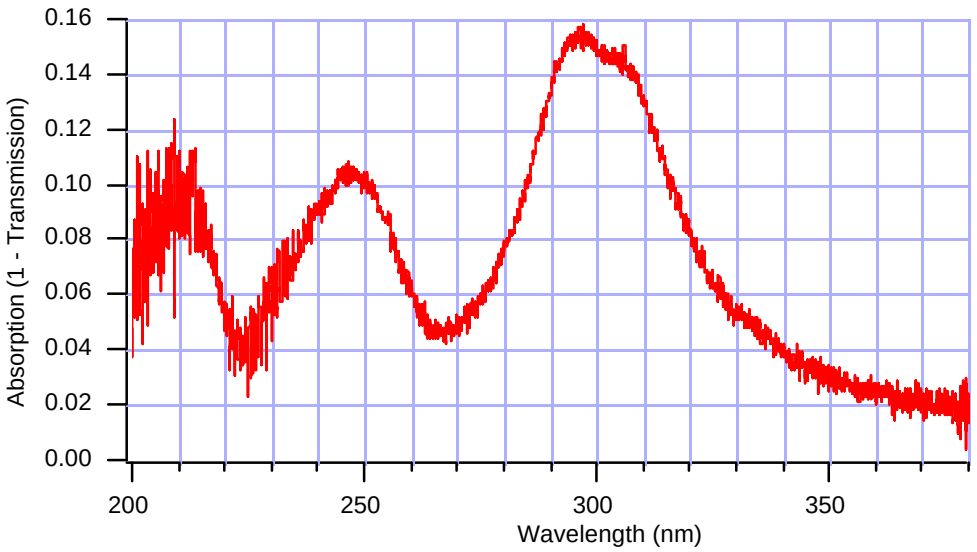

Figure 3. *Cu(THD)$_2$* Gas Absorption Spectra, 200-260 nm

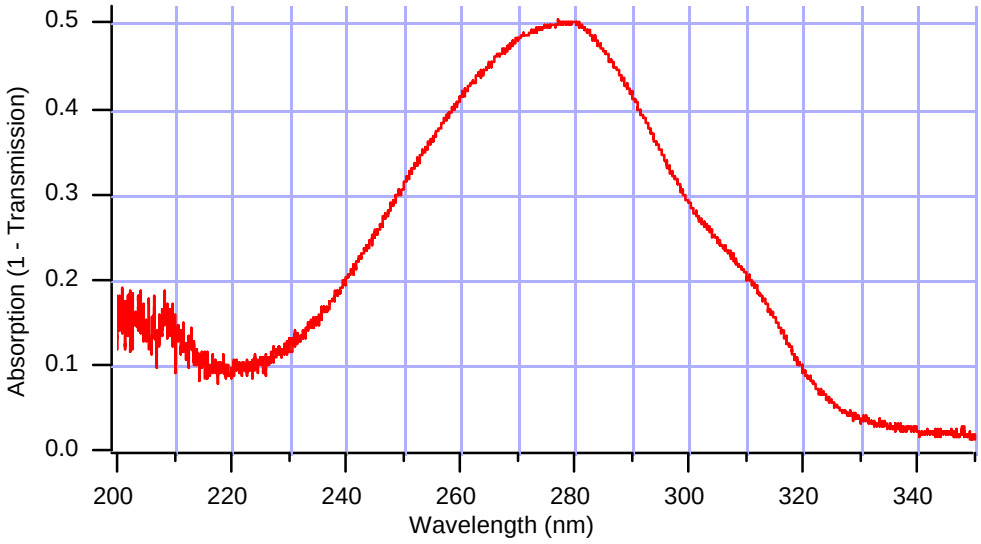

Figure 4. *Y(THD)$_3$* Gas Absorption Spectra, 200-350 nm

There are several different types of Optical Interference Methods capable of measuring thin film thickness. All of these methods evaluate the phase differences of light reflection from each interface of a thin film layer and the minimum thickness measurement possible is limited by the wavelength chosen for illumination. Generally interference methods are limited to measuring thickness of one layer on a substrate, however methods have been devised for multilayer measurements.[60] Interference techniques are also usually limited to optically transparent and isotropic films. An automated interference method has been developed that utilize CCD detection and computerized interference fringe analysis.[61]

The simplest and most common interference technique is called reflection spectrophotometry. This technique measures the amplitude of reflected light at normal incidence over a range of wavelengths. The data is then analyzed using Fresnel equations to determine film thickness. Films as thin as 30 Å can be measured relatively accurately, but best results are attained when films are greater than 200 Å thick. If the film is relatively thick, other optical parameters can be extracted from the data.

Some materials in the superconductor manufacturing process have optical constants that change throughout the deposition process. This creates a significant amount of error when measuring film thickness with reflection spectrophotometry because typically optical parameters of the film must be known *a priori*. Reflection spectrophotometry is very limited making simultaneous optical parameter measurements because of the dispersion of the index of refraction and coefficient of extinction with wavelength.[62] This technique also requires that the film surface is relatively smooth, as rough surfaces will contribute significant error to the measurement. However, despite these shortcomings, reflection spectrophotometry is an extremely robust and cost effective technique for thickness measurements when appropriate parameters are present.

Another interference technique is variable-angle reflectance measurements. In contrast to reflection spectrophotometry, measurements are made at various angles at a particular wavelength.[62] Multi-angle measurements are usually made simultaneously using a microscope objective. This technique provides greater precision and reliability then reflection spectrophotometry. It also can usually determine the thickness and index of refraction simultaneously during a measurement.[63] Variable-angle reflectance has been expanded further to include spectroscopic measurements, which have been able to resolve thickness in up to six different layers simultaneously.[64]

Ellipsometry is a another non-destructive optical technique. It is insensitive to surface irregularities and provides relatively high precision. Ellipsometry is the most sensitive technique of measuring film thickness capable of accurately measuring film thickness as thin as one Angstrom. This method can measure multiple layers of both transparent and absorbing thin films. This technique can also measure the complex index of refraction of a film and has recently been used to monitor the temperature of a film.[65] Ellipsometry is the only technique that can fully determine an anisotropic dielectric function at a particular wavelength(s).[66] This is of critical importance because superconducting cuprates such as YBCO are strongly anisotropic.

Ellipsometry measures the change in the polarization state of reflected light from a sample. More precisely, ellipsometry measures the parameters Psi and Delta, which are related to the complex reflectance coefficients by

$$r = \frac{R_p}{R_s} = \tan\Psi \exp(i\Delta)$$

Where Ψ is the amplitude ratio and Δ is the phase shift. Using a model of the film stack and corresponding Fresnel relations, the thickness of multiple layers can be determined from the ellipsometric parameters.

There are several different types of ellipsometry. Nulling or absolute ellipsometry is the simplest, most basic technique. In this technique, angular measurements are made by measuring a null signal. The optical configuration would consist of a monochromatic light source, polarizer, compensator, analyzer, and photomultiplier tube. Light passing through the polarizer and compensator becomes elliptically polarized. The elliptically polarized light is reflected off of the sample and becomes linearly polarized. The analyzer is then rotated such that the reflected light is extinguished and the photomultiplier tube measures a null signal. Although several automated nulling ellipsometry methods have been developed, the technique is cumbersome, slow and susceptible to noise.

Another ellipsometry technique, spectroscopic ellipsometry, uses a broadband light source and modulates the polarization state by rotating the polarizer, compensator or analyzer. There are several different configurations of spectroscopic ellipsometry and the particular advantages and disadvantages of each technique are beyond the scope of this study. Spectroscopic Ellipsometry has already proven itself as an effective tool for monitoring film growth[67-69] and process control[70-73] in other applications. Measurements are fast and contain a high degree of precision and repeatability. In addition to measuring film thickness, spectroscopic ellipsometry can also provide insight about the quality of a thin film superconductor by measuring the pseudodielectric function.[74] Spectroscopic ellipsometry has also been used in the laboratory to detect small changes in crystal orientation.[75]

Other variants of ellipsometry that can be used to measure film thickness include multiple-angle ellipsometry and multiple-angle spectroscopic ellipsometry. In complicated film stacks, collecting more ellipsometric data (various wavelengths, various angles) can be vital to attaining a solution for the optical parameter desired.

Picosecond Ultrasonics is a relatively new noncontact and nondestructive method of measuring thickness in thin films. In this technique, picosecond laser pulses are focused onto a region of a thin film. Absorption of the incident laser pulse creates a sudden thermal expansion, which produces an ultrasonic wave that propagates through the film. At each interface some of the sound wave is reflected back towards the surface as an echo. When an echo reaches the surface it changes the film's reflectivity. Thus the velocity of the sound wave can be measured by reflectance variations on the surface. From the velocity measurement, the thickness of the film can be determined.

Picosecond ultrasonics is best suited for opaque/metal thin films but has also been used to measure thickness in transparent thin films. [76] Measurements have a high degree of precision and repeatability as well as being extremely fast. The technique is also capable of multiple layer thickness measurements. [77] Although the technique is relatively new, commercial devices are currently available and have been deployed in the semiconductor industry. [78] Another advantage of this particular technique is that picosecond laser pulses can also be used to analyze superconducting properties of thin films. [79, 80]

Another method of thin film thickness measurement is X-Ray Diffraction. This technique has been briefly touched on the previous section on X-Ray Diffraction.

5.0 Conclusions and Recommendations

The major issues for economical manufacturing long-length YBCO-coated conductors pertain to developing a capability of continuously and uniformly depositing substrates, conductor and inerting layer coatings with correct orientation at high rates over a large area. Of course such a capability for the conductor has to meet the very important YBCO requirements of proper stoichiometric composition and epitaxial crystalline structure. For each of the potential coating methods examined, very sophisticated and quick response type diagnostics and control system will be needed to maintain a high J_c performance throughout the entire length of the conductor. On-line control systems to meet such needs are often not sufficiently developed or do not exist. Experiences from the related commercial operations, such as semiconductor fabrication, can be useful but the needs may be quite different. Therefore, parameters of importance and ways and means to monitor them on-line may need significant development efforts. That effort is on-going, in selected critical areas. Some measurement needs can use diagnostics employed in making small sample (and sometimes single crystal) conductors, but usually those diagnostics require further development to decrease evaluation time and allow rapid on-line, real time measurements.

6.0 References

1. Sheth, A. C., *et.al*., "Evaluation of Methods for Application of Epitaxial Buffer and Superconductor Layers," UTSI DOE Topical Report, DOE/PC/95231-11, March 1999.

2. Wu, X. D., *et.al*. "Properties of $YBa_2Cu_3O_{7-\delta}$ thick film on flexible buffered metallic substrates, *Applied Physics Letters*, 67 (16), October 16, 1995.

3. Goyal, A., et. al., "High Critical Current Density Superconducting Tapes by Epitaxial Deposition of $YBa_2Cu_3O_x$ Thick Films on Biaxially Textured Metals," *Applied Physics Letters*, 69, p. 1795, 1996.

4. Paranthaman, M., "Thin and Thick Film Processing of $YBa_2Cu_3O_7$ Conductors--A Brief Review," Submitted to *Supercond. Sci. and Technology*, January 31, 1996.

5. "ORNL Reports New RABiTS," *Superconductor Week Newsletter*, p. 4, March 18, 1997.

6. Leskelä, M., *et.al.*, *Chemical Vapor Deposition of High-Tc Superconducting Thin Films*, IOP Publishing Ltd., p. 628, 1993.

7. Barbe, Christophe, Ring, Terry A., "Synthesis of Superconducting Thin Films by Organometallic Decomposition," *ed*. H. C. Freyhardt, R. Flukiger, M. Peuckert, *High-Temperature Superconductors: Materials Aspects Vol. 1*, Germany: DGM, 1991.

8. Schmaderer, F., Huber, R., Oetzmann, H., Wahl, G., "Chemical Vapor Deposition of High T_c Superconductors" *ed*. H. C. Freyhardt, R. Flukiger, M. Peuckert, *High-Temperature Superconductors: Materials Aspects*, Vol. 1, Germany: DGM, 153, 1991.

8. Goyal, A., *et.al*., "High Critical Current Density Superconducting Tapes by Epitaxial Deposition of $YBa_2Cu_3O_x$ Thick Films on Biaxially Textured Metals," *Appl. Phys. Letters*, 69, p. 1795, 1996.

9. Pisch, A., Mossang, E., Weiss, F., Madar, R., Senateur, J. P., Thomas, O., "Organometallic chemical vapor deposition of superconducting Y-Ba-Cu-O films," *ed*. H. C. Freyhardt, R. Flukiger, M. Peuckert, *High-Temperature Superconductors: Materials Aspects Vol. I*, Germany: DGM, 1991.

10. Singh, R., Sinha, S., Hsu, N. J., Chou, P., "Superconducting thin films of Y-Ba-Cu-O prepared by metalorganic chemical vapor deposition," *Journal of Applied Physics*, 67, p. 1562, 1990.

11. Terada, N. *et.al.*, "Surface Study of $YBa_2Cu_3O_{7-\delta}$ Epitaxial Films Cleaned by an Atomic Oxygen Beam," *Applied Physics Letters*, 64, p. 2581, 1994.

12. Zhang, J., *et.al.*, "Single Liquid Source Plasma-Enhanced Metalorganic Chemical Vapor Deposition of High-Quality $YBa_2Cu_3O_{7-x}$ Thin Films," *Appl. Phys. Letters*, 61 (24), pp. 2884-2886, Dec. 1992.

13. Blanchet, G. B. and Fincher, C. R., Jr., "High Temperature Deposition of HTSC Thin Films by Spray *Supercond. Sci. Technol*., 4, pp. 69-72, 1991.

14. Kawai, Maki, et. al., "Formation of Y-Ba-Cu-O Superconducting Film by a Spray Pyrolysis Method," *Japanese Journal of Applied Physics*, 26, No. 10, L1740-L1742, Oct. 1987.

15. Leskelä, M., Truman, J. K., Mueller, C. H., Holloway, P. H., "Preparation of superconducting Y-Ba-Cu-O films," *Journal of Vacuum Science Technology, A: Vacuum, Surfaces, and Films*, 7, p. 3147, 1989.

16. Rossnagel, S. M. and Cuomo, J. J., *AIP Conference Proceedings*, 165, p. 106,1987.

17. Ottosson, M., et. al., “Chemical Vapor Deposition of the Superconducting $YBa_2Cu_3O_{7-x}$ Phase Using Halides as Metal Sources,” *Appl. Phys. Letter*, 54 (24), pp. 2476-2478, June 1989.

18. Abolmaali, S. B. and Talbot, J. B., “Synthesis of Superconductive Thin Films of $YBa_2Cu_3O_{7-x}$ by a Non-Aqueous Electrodeposition Process,” *J. Electrochem. Soc.*, 140, (2), pp. 443-445, Feb. 1993.

19. Hein, M., Kraut, S., Müller, G., Opie, D., Piel, H., Ponto, L., Wehler, K., "Fabrication of textured $Y_1Ba_2Cu_3O_{7-x}$ layers by electrophoresis," *ed*. H. C. Freyhardt, R. Flukiger, M. Peuckert, *High-Temperature Superconductors: Materials Aspects Vol. I*, Germany: DGM, 147, 1991.

20. Iijima, Y., Tanabe, N., Kohno, I., Ikeno, Y., "In-plane aligned $YBa_2Cu_3O_{7-x}$ thin films deposited on polycrystalline metallic substrates," *Applied Physics Letters*, 60, 769, 1992.

21. Hammond, R. H., “Thick Film YBCO for Wires and Tapes: Scale-Up Issues and Cost Estimates,” Proceedings of the 8th International Symposium on Superconductivity (ISS ‘95), published as *Advances in Superconductivity VIII*, *ed.* M. Hayakawa and Y. Enomoto, Springer-Verlag, Tokyo, 1996.

22. Wang, Weizhi, Hammond, R. H., Fejer, M. M., Ahn, C. H., Beasley, M. R., Levenson, M. D., Bortz, M. L., "Diode-laser-based atomic absorption monitor using frequency-modulation spectroscopy for physical vapor deposition process control," *Applied Physics Letters*, 67, p. 1375, 1995.

23. Gnanarajan, S., Katsaros, A., Savvides, N., "Biaxially aligned buffer layers of cerium oxide, yttria stabilized zirconia and their bilayers," *Applied Physics Letters*, 70, p. 2816, 1997.

24. Matijasevic, V., Rosenthal, P., Shinohara, K., Marshall, A. F., Hammond, R. H., Beasley, M. R., “Reactive Co-Evaporation of YBaCuO Superconducting Films,” *Journal of Materials Research*, 6, p. 682, 1991.

25. McIntyre, P. C., *et.al.*, “Effect of Growth Conditions on the Properties and Morphology of Chemically Derived Epitaxial Thin Films of Ba_2 Y Cu_3 O_{7-x} on (001) $LaAlO_3$,” *J. Appl. Phys*., 71 (4), pp. 1868-1877, Feb. 1992.

26. Ram, P., Saxena, V.R., and Ramamohan, T.R., "Densification and High Critical Current Densities in Bulk $YBa_2Cu_3O_{7-y}$ Superconductor by the State Reaction Technique," *Materials Science and Engineering B*, B34, p. 106, 1995.

27. Norton, D. P., Goyal, A., et. al. "Epitaxial $YBa_2Cu_3O_7$ on Biaxially Textured Nickel (001) : An Approach to Superconducting Tapes with High Critical Current Density," *Science*, 274, p. 755, 1996.

28. Göres, J., Pang-Jen Kung, Fenner, D. B., and Budnick, J. I., "In situ Plume-Emission Monitoring During Pulsed-Laser Deposition of $YBa_2Cu_3O_{7-\delta}$ and Yttria-Stabilized Zirconia Thin Films, " *Review of Scientific Instruments*, 68, p. 170, 1997.

29. Skofronick, G. L., Carim, A. H., Foltyn, S. R., and Muenchausen, R. E., "Orientation of $YBa_2Cu_3O_{7-x}$ Films on Unbuffered and CeO_2-Buffered Yttria-Stabilized Zirconia Substrates," *Journal of Applied Physics*, 76, p. 4753, 1994.

30. G. Brorsson, G., Olsson, E., *et.al*. , "$YBa_2Cu_3O_{7-x}$ Films on Yttria-Stabilized ZrO_2 Substrates : Influence of the Substrate Morphology," *Journal of Applied Physics*, 75, p. 7958, 1994.

31. Greer, J. A., "High quality YBCO films grown over large areas by pulsed laser deposition," *Journal of Vacuum Science and Technology, A: Vacuum, Surfaces, and Films*, 10, p. 1821, 1992.

32. Shoup, S. S, *et.al*., "Sol-gel Synthesis of $LaAlO_3$; Epitaxial Growth of $LaAlO_3$ Thin Films on $SrTiO_3$ (100)", Submitted for publication in *J. Material Sci.*, Oak Ridge National Laboratory, Feb. 1996.

33. Rupich, M. W., *et.al.*, "Low-Temperature Formation of $YBa_2Cu_3O_{7-x}$ Superconducting Films From Molecular Cu-Ba-Y Precursors," *Appl. Phys. Letters*, 60 (11), pp. 1384-1386, March 1992.

34. Budai, J. D., Reenstra, R. and Boatner, L. A., "X-Ray Study of In-plane Epitaxy of $Yba_2Cu_3O_x$ Thin Films," *Physical Review B*, 39 (16), June 1989,12355-12358

35. Lagally, M.G., Savage, D.E., and Tringides, M.C. NATO ASI Series, Series B, Physics, New York, Plenum Press with NATO Scientific Affairs Div., pp. 139-174, 1990.

36. Rijnders, G., Koster, G., Blank, D. and Rogalla, H., "*In-Situ* Monitoring During Pulsed Laser Deposition of Complex Oxides Using Reflection High Energy Electron Diffraction Under High Oxygen Pressure," *Appl. Phys. Lett*., 70 (14), p 1888-1890, April 1997.

37. Blank, D. and Rogalla, H., "*In-Situ* Diagnostics at High Pressures: Ellipsometric and RHEED Studies of the Growth of $Yba_2Cu_3O_7$," Presented at the Materials Research Society Fall Meeting, 1997.

38. Atwater, H. A., *et. al.,* Analysis of Monolayer Films During Molecular–Beam Epitaxy by Reflection Electron Energy Loss Spectroscopy," *Surface Science,* 1993.

39. Muller, D. A., "New Strategies for Atomic Scale Measurements at Interfaces using Electron Energy Loss Spectroscopy," Presented at the American Physics Society March Meeting, 1997.

40. Bhadra, R., *et.al.*, "Raman scattering from high-T_c superconductors," *Physical Review B*, 37, p. 5142, 1988.

41. Krol, D. M., *et.al.*, "Raman spectroscopy of single crystals of high-T_c cuprates," *Journal of Optical Society of America*, 6, p. 448, 1989.

42. Sodtke, Erik, Munder, Herbert, "Oxygen content and disorder in a-axis oriented $YBa_2Cu_3O_{7-x}$ thin films," *Applied Physics Letters*, 60, p. 1630, 1992.

43. Gasparov, L. V., *et.al.*, "Phonon-mode characterization of orthorombic and tetragonal YBa_2Cu_3O7-x single crystals by Raman spectroscopy," *Journal of the Optical Society of America*, 6, p. 440, 1989.

44. Zheng, Jia-qi, *et.al*., "Study of high-T_c superconducting YBaCuO thin films," *Solid State Communications*, 65, p. 59, 1988.

45. Zhang, P., Haage, T, Habermeier, U. -U., Ruf, T., Cardona, M., "Raman spectra of ultrathin $YBaCuO_{7-x}$ films," *Journal of Applied Physics*, 80, p. 2935, 1996.

46. Hopkins, J.B., Farrow, L. A., "Raman microprobe determination of local crystal orientation," *Journal of Applied Physics*, 59, p. 1103, 1986.

47. Jahanzeb, A. *et.al.*, "Studies and implications of the Hall effect in superconducting and semiconducting $YBa_2Cu_3O_{7-x}$ thin films," *Journal of Applied Physics*, 78, p. 6658, 1995.

48. Karmanenko, S.F., *et.al.*, "Influence of the growth rate of $YBa_2Cu_3O_{7-x}$ films on the orientation of the crystallographic axes," *Technical Physics Letters*, 22, p. 982, 1996.

49. Belousov, M. V., *et.al.*, "Raman scattering of light used as a method of analyzing the oriented $YBa_2Cu_3O_{7-x}$ films," *JETP Letters*, 48, p. 316, 1989.

50. Karmanenko, S. F., “Influence of growth rate on the structural orientation of YBCO superconducting *Supercond. Sci. Technol.* 12, pp. 36-44, 1999.

51. Aleksandrov, I. V. *et.al*., “Raman scattering in single crystals of $YBa_2Cu_3O_x$ high- temperature superconductors”, *JETP Letters*, 47, p. 223, 1988.

52. Gores, J., Kung, Pang-Jen, Fenner, D. B., Budnick, J. I., “*In Situ* Plume-Emission Monitoring During Pulsed-Laser Deposition Of $YBa_2Cu_3O_{7-x}$ and Yttria-Stabilized Zirconia Thin Films,” *Rev. Sci. Instrum.*, 68 (1), p. 170, 1997.

53. Clark, G. J., Frost, T. and Russell, M. A. (*ed*.), *UV Spectroscopy: Techniques, Instrumentation, Data Handling*, Chapman & Hall, London, 1993.

54. Svanberg, S., *Atomic and Molecular Spectroscopy, Basic Aspects and Practical Applications*, (second edition) Springer Verlag, New York 1992, 1992.

55. Calcium: Method 215.1 (atomic absorption, direct aspiration) pp. 215.1-215.2. In “Methods for Chemical Analysis of Water and Wastes,” United States Environmental Protection Agency Report EPA-600/4-79-020, Cincinnati, OH, 1983.

56. Kliger, D. S., (*ed.*) *Ultra Sensitive Laser Spectroscopy*, Academic Press, New York, 1983.

57. Harima, H., Ohnishi, H., Hanaoka, K., Tachibana, K., and Goto, Y., “An IR Study on the Stability of Y(DPM)3, Ba(DPM)2, and Cu(DPM)2 for UV Irradiation,” *Japanese Journal of Applied Physics*, 30 (9A) pp. 1946-1955, Sept. 1991.

58. Rappoli, B. J. and DeSisto, W. J., “Gas Phase Ultraviolet Spectroscopy of High-Temperature Superconductor Precursors for Chemical Vapor Deposition Processing,” *Applied Physics Letters*, 68 (19) pp. 2726-2728, May 1996.

59. Thomas, M. E., “An Evaluation of Absorption Spectroscopy to Monitor Yba2Cu3O7-x Precursors for Metal Organics Chemical Vapor Deposition Processing, DOE/PC/95231-23, Thesis, University of Tennessee, May 1999.

60. Alius, H. and Schmidt, R., “Interference method for monitoring the refractive index and the thickness *Rev. of Sci. Instr*., 61, (4), pp. 1200-1203, 1990.

61. Gonzalez, A. and Bernabeu, E., “Automatic interference method for measuring transparent film thickness”, *Appl. Opt*., 32, (13), p. 1, 1993.

62. Rosencwaig, A., Opsal, J., Willenborg, D. L., Kelso, S. M. and Fanton, J. T., “Beam Profile reflectometry: A new technique for dielectric film measurements”, *Appl. Phys. Lett*. 60, (11), 1992.

63. Fanton, J. T., Opsal, J., Willenborg, D. L., Kelso, S. M. and Rosencwaig, A., “Multiparameter measurements of thin films using beam-profile reflectometry”, *J. Appl. Phys*, 73 (11), p. 1, 1993.

64. Leng, J. M., Sidorowich, J. J., Yoon, Y. D. and Opsal, J., “Simultaneous measurement of six layers in a silicon on insulator film stack using spectrophotometry and beam profile reflectometry”, *J. Appl. Phys*., 81 (8), p. 15, April 1997.

65. Jiang, Z.-T., Yamaguchi, T., Aoyama, M., and Hayashi, T., “Possibility of simultaneous monitoring of temperature and surface layer thickness of Si substrate by *in situ* spectroscopic ellipsometry”, *Japanese Journal of Applied Physics*, Part 1: Regular Papers, Short Notes & Review Papers, 37, (2), pp. 479-483, Feb. 1998.

66. Burau, A., Weber, H. J. and Pavlov, V. V., "Determination of the Dielectric Function of Strongly Anisotropic Crystals in Reflection," *J. Opt. Soc. Am. A*, 13, (1), Jan 1996.

67. Urban, F. III and Comfort, J. C. "Numerical Ellipsometry: Applications Of A New Algorithm For Real-Time, *In-Situ* Film Growth Monitoring", *Journal of Vacuum Science & Technology A: Vacuum, Surfaces, and Films*, 14, (4), pp. 2331-2336, July 1996.

68. An, I., Nguyen, H. V., Heyd, A. R. and Collins, R. W., "Simultaneous Real-Time Spectroscopic Ellipsometry And Reflectance For Monitoring Thin-Film Preparation", *Rev. of Sci. Instr*., 65, (11), pp. 3489-3500, Nov. 1994.

69. Kildemo, M. and Drevillon, B., "Real Time Monitoring Of The Growth Of Transparent Thin Films By Spectroscopic Ellipsometry", *Appl. Phys. Lett*., 67, (7), pp. 918-920, Aug. 1995.

70. Duncan, W. M., Henck, S. A., Kuehne, J. W., Loewenstein, L. M. and Maung, S., "High-Speed Spectral Ellipsometry For *In-Situ* Diagnostics And Process Control", *Journal of Vacuum Science & Technology B: Microelectronics and Nanometer Structures*, 12, (4), pp. 2779-2784, July 1994.

71. Kildemo, M., Brenot, R. and Drevillon, B. "Spectroellipsometric Method For Process Monitoring Semiconductor Thin Films and Interfaces", *Applied Optics*, 37, (22), pp. 5145-5149, Aug. 1998.

72. Henck, S., "*In-Situ* Real-Time Ellipsometry for Film Thickness Measurement and Control", *J. of Vacuum Science & Technology A: Vacuum, Surfaces, and Films*, 10, (4), pp. 939-938, July 1992.

73. Hayashi, Y. and Itoh, A., "Ellipsometric Monitor for Process Control", *Appl. Optics*, 28, (4), pp. 703-707, Feb. 1989.

74. Garriga, M., Humlicek, J., Barth, J., Johnson, R. L. and. Cardona, M, "Ellipsometric Measurements of High-T_c Compounds", *J. Opt. Soc. Am. B*, 6, (3), March 1989.

75. Sengupta, L. C., Huang, D., Roughani, B., Aubel, J. L., Sandaram, S. and Chang, C. L., "Spectroscopic Ellipsometry Studies of $YBa_2Cu_3O_{7-\delta}$ Depositing on $SrTiO_3$", *J. of Appl. Phys*., 69, (12), pp. 8272-8276, June 1991.

76. Wright, O.B., "Thickness and Sound Velocity Measurement in Thin Transparent Films with Laser *J. of Appl. Phys*., 71, (4), pp. 1617-1629, Feb 1992.

77. Morath, C. J., Collins, G. J., Wolf, R. G. and Stoner, R. J., "Ultrasonic Multilayer Metal Film *Solid State Technology*, June 1997.

78. MetaPULSE 300, http://www.rudolphtech.com/products/product_meta300.html, product literature of Rudolph Technologies Inc., 1997

79. Shi, L., Huang, G. L., Lehane, C., Kim, D., Kwok, H.S., Swiatkiewicz, J., Xu, G. C. and Prasad, P.N. "Picosecond Photoresponse in Y-Ba-Cu-O Ultrathin Films", *Phys. Rev. B*, 48, (9), pp. 6550-6555, Sept. 1993.

80. Sobolewski, R., Butler, D. P., Hsiang, T. Y. and Stancampiano, C. V., "Dynamics of the Inter-mediate State in Nonequilibrium Superconductors," *Phys. Rev. B*, 33, (7), pp. 4604-4614, 1986.